

# Journal of Materials Chemistry A

Accepted Manuscript



This is an *Accepted Manuscript*, which has been through the Royal Society of Chemistry peer review process and has been accepted for publication.

*Accepted Manuscripts* are published online shortly after acceptance, before technical editing, formatting and proof reading. Using this free service, authors can make their results available to the community, in citable form, before we publish the edited article. We will replace this *Accepted Manuscript* with the edited and formatted *Advance Article* as soon as it is available.

You can find more information about *Accepted Manuscripts* in the [Information for Authors](#).

Please note that technical editing may introduce minor changes to the text and/or graphics, which may alter content. The journal's standard [Terms & Conditions](#) and the [Ethical guidelines](#) still apply. In no event shall the Royal Society of Chemistry be held responsible for any errors or omissions in this *Accepted Manuscript* or any consequences arising from the use of any information it contains.

Cite this: DOI: 10.1039/c0xx00000x

www.rsc.org/xxxxxx

ARTICLE TYPE

# Efficient synthesis of hierarchical NiO nanosheets for high-performance flexible all-solid-state supercapacitor

Yue Qian,<sup>a</sup> Rong Liu,<sup>a</sup> Qiufan Wang,<sup>a</sup> Jing Xu,<sup>a</sup> Di Chen<sup>\*a</sup> and Guozhen Shen<sup>\*b</sup>*Received (in XXX, XXX) Xth XXXXXXXXX 20XX, Accepted Xth XXXXXXXXX 20XX*

5 DOI: 10.1039/b000000x

Hierarchical NiO nanosheets were successfully grown on flexible carbon fibers with pre-deposited ZnO nanoparticle films as the buffer layers, followed with the removal of the ZnO films. The as-grown NiO nanosheets with excellent flexibility exhibited a largest specific capacitance of 842 mF/cm<sup>2</sup> at a current density of 1 mA/cm<sup>2</sup>. Configured as flexible symmetric all-solid-state supercapacitors, the device showed 10 a specific capacitance of 20 mF/cm<sup>2</sup> at 0.1 mA/cm<sup>2</sup>, excellent cyclability with a real capacitance of about 20 mF/cm<sup>2</sup> ever over 10000 cycles, and excellent mechanical flexibility and stability under different curvatures.

## Introduction

Flexible energy storage devices have attracted considerable 15 attention in the past few years for their novel functions in comparison to conventional energy storage devices. As one of the most important energy storage devices, supercapacitors (SCs) have been widely used in portable electronics, power back-up, electrical vehicles and various microdevices, owing to 20 their properties of high power density, long cycle lifetime, excellent charge-discharge and environment friendly characteristics.<sup>1,2</sup> Also, they can provide an instantaneously higher power density than lithium ion batteries and higher energy density than conventional dielectric capacitors.<sup>3,4</sup> To 25 better meet the rapid growing modern market demands, abundant efforts have been dedicated to achieve thin, lightweight, flexible and even rollup SCs with a variety of structures for next generation all-in-one portable and wearable electronics.<sup>5-13</sup>

30 Carbon cloth with high electrical conductivity and excellent flexibility has been widely adopted as substrates for flexible energy storage devices. Several kinds of nanostructured electrodes, such as Fe<sub>3</sub>O<sub>4</sub>, ZnCo<sub>2</sub>O<sub>4</sub>, NiCo<sub>2</sub>O<sub>4</sub>, etc have been successfully grown on carbon cloth. With high electrical 35 conductivity and an outstanding theoretical specific capacitance of 2573 F/g, nickel oxide (NiO) nanostructures are considered as promising candidates for flexible SCs.<sup>14-16</sup> If NiO nanostructures are directly grown on carbon cloth, flexible SCs with improved performance should be fulfilled. Unfortunately, 40 due to the smooth surface of carbon cloth, the weak adsorbability and the superhydrophilic surface state of the Ni(OH)<sub>2</sub> precursor during solution process, it is usually hard to directly grow NiO nanostructures on the C cloth with acceptable uniformity.

45 In this paper, we develop a simple strategy to grown NiO nanosheets on carbon cloth, which are used as a binder-free electrode for high-performance flexible supercapacitors.

During this process, ZnO nanoparticle films were first deposited on carbon cloth and act as a buffer layer for the 50 following NiO growth. Configured as all-solid-state SCs, the as-fabricated NiO-based flexible device showed specific capacitance, specific energy and low leakage of 21 mF/cm<sup>2</sup>, 0.322 mWh/cm<sup>3</sup> and 4.66 μA, respectively. Moreover, the cell electrochemical performances were well retained at different 55 curvatures, indicating excellent mechanical flexibility and stability.

## Experimental section

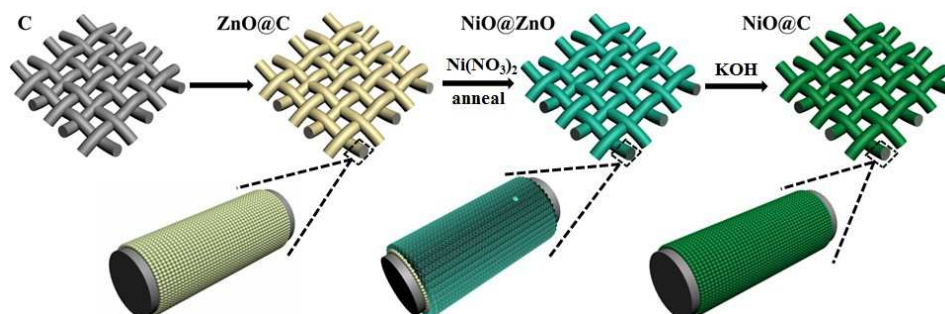
Scheme 1 shows the typical experimental process for the growth of NiO nanosheets on carbon cloth (NiO@C cloth). 60 During this process, a layer of ZnO nanoparticles films were first grown on carbon cloth via a hydrothermal method according to our previous report.<sup>17</sup> To grow NiO nanostructures on carbon cloth, the pre-prepared ZnO@C cloth was first immersed into 0.1 M Ni (NO<sub>3</sub>)<sub>2</sub> aqueous solution at 65 80 °C for 6 h. After cooling down to room temperature, the samples were annealed at 400 °C for 2 h, which were then soaked in 2 M KOH aqueous solution for 3 h to remove ZnO buffer layer.

Field emission scanning electron microscopy (FESEM, 70 Sirion 200, FEI, The Netherlands) was used to characterize the morphologies of products. The chemical composition was investigated by the X-ray powder diffraction patterns (XRD, X'Pert PRO, PANalytical B.V., The Netherlands).

The electrochemical properties of the NiO@C cloth 75 electrode was first studied in a typical three-electrode system, with the NiO@C cloth as the working electrode, a platinum foil as the counter electrode and an SCE as the reference electrode in the electrolyte of 3 M KOH aqueous solution. The flexible all-solid-state SCs were fabricated following a typical 80 procedure: 6 g of PVA was added into 50 mL of deionized water with continuously stirring at 90 °C. Until the PVA was

dissolved completely, 4 g of KOH in 10 ml of water was added. Two strips of obtained NiO@C cloth were immersed into the gel electrolyte with the same size, keeping the electrodes part above the solution. After the gel electrolyte solidified at room

temperature, the two strips were assembled in the final device with sandwiched structures. All electrochemical measurements were performed with an electrochemical workstation (CHI706D, Shanghai, China).



Scheme 1. Schematic illustration for the synthesis procedure of NiO nanosheets on carbon cloth.

## Results and discussion

Figure 1a shows the SEM image of the ZnO-coated carbon fibers from the hydrothermal process. After immersed in Ni (NO<sub>3</sub>)<sub>2</sub> solution and high temperature treatment, a layer of NiO nanosheets were found deposited uniformly on the ZnO-coated carbon fibers, as shown in Figure 1b. From the inset image in Figure 1b, we can see that these NiO nanosheets form into uniform hierarchical structure. After immersed the cloth into KOH aqueous solution for 3 h, ZnO particles were successfully removed, resulted in the formation of pure NiO nanosheets, according to the SEM image in Figure 1c and the XRD pattern in Figure 1d. It should be mentioned although the NiO structure was a little destroyed after removal of ZnO nanoparticles, the hierarchical structure was still kept as can be seen from inset in Figure 1c. Compared with the product synthesized from pure carbon cloth without ZnO buffer layer (Supporting information, Figure S1), the product with the ZnO buffer layer is quite uniform, indicating the important role of ZnO buffer layer for the growth of NiO nanostructures on carbon cloth. From the black curve to the red and then to the blue one in the XRD patterns, the evolution of materials on carbon cloth were revealed incisively and vividly from pure ZnO to ZnO/NiO, and finally NiO phases.

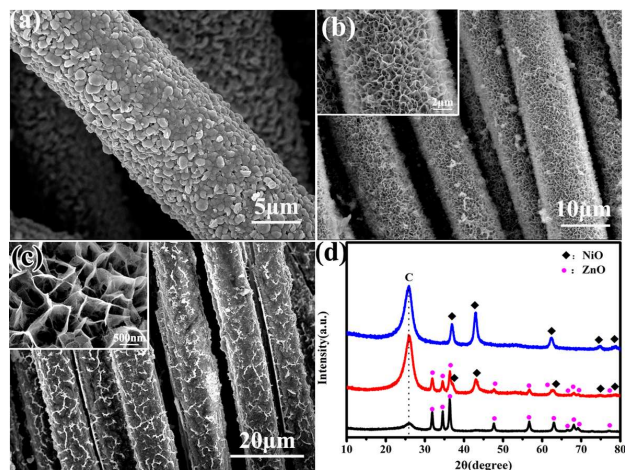


Figure 1. SEM images of the products obtained at various processes: (a) ZnO @ C cloth, (b) NiO @ ZnO on carbon cloth and (c) NiO @ C cloth. (d) The corresponding XRD patterns.

The electrochemical properties of the as-grown electrodes

were first measured in a three-electrode cell. Figure 2a shows the cyclic voltammetry (CV) curves of the NiO@C cloth, NiO@ZnO on carbon cloth, ZnO@C cloth and C cloth electrodes in a potential range of 0 to 0.5 V at a constant scan rate of 10 mV/s, respectively. It can be distinctly seen that all CV curves exhibit a pair of redox peaks except the pure C cloths, implying that carbon cloth contributes little to the capacitance. Besides, the CV integrated area of the NiO@C cloth electrode is larger than that of the NiO@ZnO on carbon cloth and the ZnO@C cloth, suggesting that the NiO@C cloth electrode has the best pseudocapacitive characteristic.<sup>9, 16,18</sup>

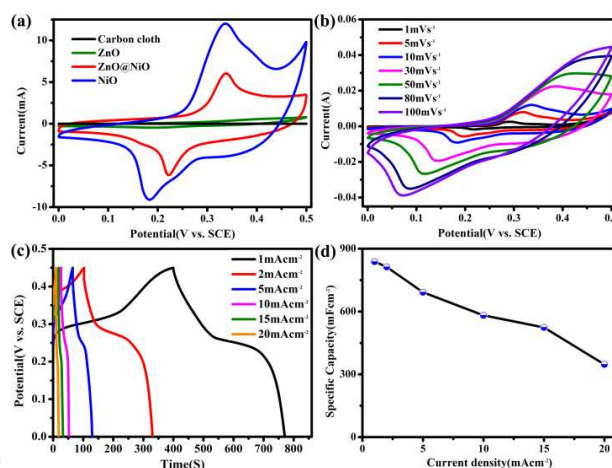


Figure 2. (a) Cyclic voltammograms of NiO@C cloth, NiO@ZnO on carbon cloth, ZnO@C cloth and C cloth electrodes in a potential range of 0 to 0.5 V at a constant scan rate of 10 mV/s. (b) Cyclic voltammograms of NiO@C cloth at different scan rates with potential windows ranging from 0 to 0.5 V. (c) Constant current charge/discharge curves for NiO@C cloth composite electrode at various current densities in the potential range 0-0.45 V. (d) Specific capacitances of the NiO@C cloth electrode at different current densities.

Figure 2b presents the CV curves of the NiO@C cloth at different scan rates. Clearly, all the CV curves of the NiO@C cloth electrode show a pair of Faradaic redox peaks (~0.22 V and 0.3 V) at the scan rate of 1 mV/s. With increased scan rates, the current response increases accordingly and the shapes of the CV curves are well kept, indicating the good capacitive behavior and high-rate capability of the electrode.<sup>7,8,19</sup> According to previous reports, the redox peaks are mainly

related to the following reversible redox reaction:



Constant current charge/discharge curves for the NiO@C cloth electrode at various current densities in the potential range of 0-0.45 V were shown in Figure 2c. The typical capacitance of the electrode can be calculated according to the following equation:

$$C_{\text{area}} = I * \Delta t / (\Delta V * S) \quad (2)$$

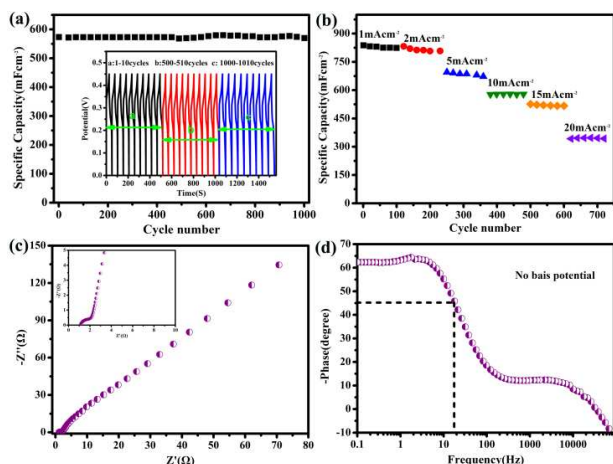


**Figure 3.** Electrochemical performance of NiO@C cloth device: (a) Galvanostatic charge/discharge cycling stability of a NiO@C cloth supercapacitor device over 1000 cycles at 10 mA/cm<sup>2</sup>. The inset was the first 10 charge/discharge cycles, the middle 10 cycles and the last 10 cycles curve after 1000 cycles. (b) Cycling performance for NiO@C cloth at different current densities. (c) Nyquist impedance plots of the NiO@C cloth device. (d) Bode plot showing phase angle vs. frequency for a typical electrochemical capacitor.

Where  $I$  is the constant discharge current,  $S$  is the geometrical area of the electrode,  $\Delta t$  is the discharged time after  $IR$  drop, and  $\Delta V$  is the voltage drop upon discharge, respectively. A specific capacitance of 842 mF/cm<sup>2</sup> was obtained for the electrode at the charge/discharge current density of 1 mA/cm<sup>2</sup>.

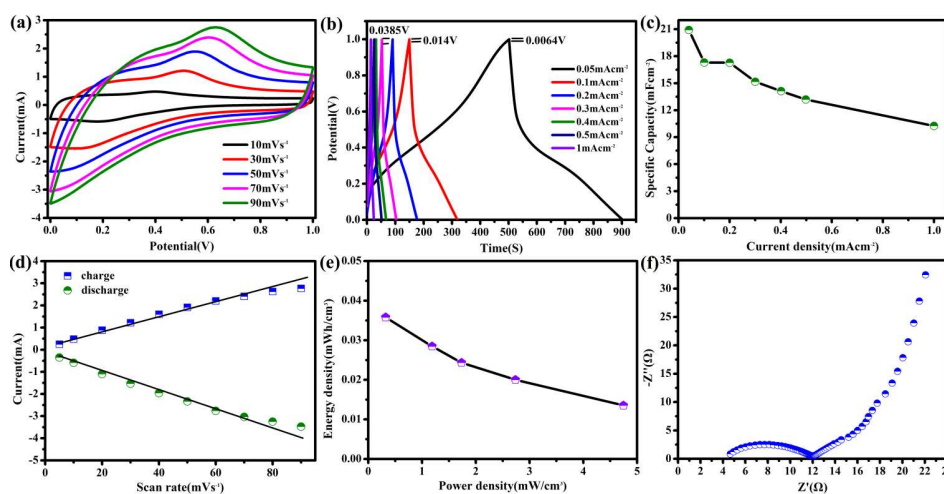


**Figure 4.** (a) The CV curves of flexible SC device at different scan rates. (b) The galvanostatic charge/discharge curves at different current densities. (c) The specific electrode capacitance of the flexible cloth devices as a function of the current density. (d) Evolution of the charge and discharge current density versus scan rate. (e) Ragone plot (power density vs. energy density). (f) The impedance spectra for the flexible device.

The charge/discharge curves and cycling performance of the

Compared with previous reported oxide nanostructures electrodes, our samples here exhibited considerably higher specific capacitance.<sup>7,20,21</sup> Even at a relatively high current density of 20 mA/cm<sup>2</sup>, the specific capacitance of as high as 350 mF/cm<sup>2</sup> can still be achieved. At the current density of 1 mA/cm<sup>2</sup>, no obvious  $IR$  drop was observed at the beginning of the discharge curve, suggesting a low internal resistance of the electrode.

For a comparison, the charge/discharge curves of the NiO@ZnO based electrode were also measured and the result is shown in Figure S2b, revealing that no obvious component synergistic effects between NiO and ZnO. According to the equation 2, the specific capacitance of the NiO@C cloth electrode can be calculated to be 842, 814, 694.7, 582, 523.8, and 350 mF/cm<sup>2</sup> at current densities of 1, 2, 5, 10, 15 and 20 mA/cm<sup>2</sup>, respectively. The corresponding result is shown in Figure 2d. It can be concluded that the surface area modification of carbon cloths by NiO sheets has a strong influence on the enhancement of capacitance, as larger specific surface area will promote ion diffusion in the NiO@C cloth device.

The long-term cycling performance of the NiO@C cloth electrode in a potential window of 0-0.45 V was measured by the consecutive galvanostatic charge/discharge at current density of 10 mA/cm<sup>2</sup>, and the result is given in Figure 3a. The first 10 cycles, the middle 10 cycles and the last 10 cycles of the charge-discharge electrochemical stability are also given in the inset picture of Figure 3(a). From the curves of the last 10 cycles, the capacitance was still remained as high as 97% of the initial 10 cycles, which shows a stable electrochemical performance than previously reported results.<sup>20,24,25</sup> The result of the continuous charge/discharge measurements exhibits a good reversible characteristic of the electrode without any apparent deviation. Figures S2c-2d shows the SEM image and XRD pattern of the NiO@C cloth electrode after cycled for 1000 times, which still maintained the initial structure, indicating the good stability of the electrode.

65 NiO@C cloth electrode at different current densities (1, 2, 5,

10, 15, 20 mA/cm<sup>2</sup>) between 0 and 0.45 V (vs. SCE) are shown in Figure 3b. From which we can see that increasing the current density from 1 mA/cm<sup>2</sup> to 20 mA/cm<sup>2</sup> resulted in a reduction of the capacity from 830 mF/cm<sup>2</sup> to 347 mF/cm<sup>2</sup>, while the stable cycling performance at each current density is still maintained, further confirming the stability of the electrode.

The electrochemical impedance spectroscopy (EIS) is a non-destructive and useful technique for evaluating the kinetic and mechanistic information of electrode materials. The Nyquist plot with an enlarged view in the inset of the impedance data is shown in Figure 3c. The plots consist of two distinct parts, including a semicircle at high-frequency followed by a linear component at the low-frequency. The high-frequency is related to Faradic reactions, and a linear line at low-frequency shows a Warburg impedance related to the diffusion of electrolyte within the pores of the electrode.<sup>13,26,27</sup> As shown in Figure 3c, the intercept of the Nyquist curve on the real axis is about 1.1 Ω, manifesting the good conductivity of the electrolyte and very low internal resistance of the electrode.<sup>1</sup>

The impedance phase angle plot is shown in Figure 3d. The frequency  $f_0$  at the phase angle of -45° is about 17.18 Hz, which marks the point where the resistive and capacitive impedances are equal. The  $f_0$  provides a relaxation time constant  $\tau=0.058s$  ( $\tau=1/f_0$ ), that tells how fast the device can be reversibly charged and discharged.<sup>2,28,29</sup> In the phase angle plot, the approaching to a more capacitive behavior at low frequency is usually identified with the phase angle approaching to the negative 90°. Therefore, the value of the phase angle is used to evaluate the effectiveness of ion diffusion in mesopores. That is, the smaller the phase angle, the better the capacitive performance and the faster the ions diffusion.

NiO materials applied in all-solid-state supercapacitors have rarely been reported until now. Herein, a flexible all-solid-state SC was then fabricated by using the as-grown NiO@C cloth as the electrodes. Figure 4a presents the CV curves of the flexible SC at the scan rates range from 10 mV/s to 90 mV/s with a potential window between 0 and 1 V. The quasi-rectangular shape of CV curves indicates the device behavior with very rapid current response on voltage reversal.<sup>9,30</sup> The charge/discharge behavior of the flexible device at different current densities is shown in Figure 4b. From the curves, we can clearly see that the voltage drop of the discharge part become larger with the increased current density. The near triangle-like curves demonstrate the good capacitive behavior and electrochemical reversibility of the device.<sup>31-33</sup> The corresponding specific capacitances of the device are calculated according to the same formula with the three-electrodes and the results were shown in Figure 4c. At slower scan rates, the diffusion of ions from the electrolyte can gain access to almost all available pores of the film electrodes and the penetration of electrolytic ions into the pores will be a lot deeper, leading to a higher specific capacitance.

Furthermore, a linear dependence of the charge and discharge current at the scan rate almost up to 70 mV/s can be observed in Figure 4d. The deviation of the linear dependence after 70 mV/s is mainly due to the diffusion limit of the gel electrolyte ions to the electrode materials. The linear of charge current is symmetric with the linear of discharge current, which

indicated the NiO@C based all-solid-state device owns excellent reversibility.<sup>34-36</sup>

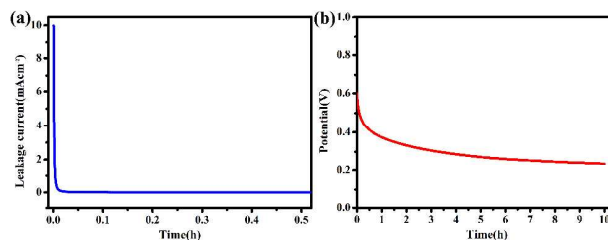


**Figure 5.** (a) Leakage current curves of the flexible all-solid state device over 0.5h. (b) Self-discharge curves of the device after charging at 1 V.

Figure 4(e) shows the Ragone plot (power density vs energy density) of the NiO@C cloth based device. The power density and energy density are calculated from the following equations:

$$E=CV^2/(2U) \quad (3)$$

$$P=E/t \quad (4)$$

Where  $C$  is total capacitance of the device,  $V$  is the cell voltage,  $U$  is the device volume, and  $t$  is the discharge time. According to the specific capacitance in Figure 3c, under the calculation of formula 3 and 4, a high energy density of 0.322 mWh/cm<sup>3</sup> was achieved.<sup>6,10</sup>

Electrochemical impedance spectroscopy (EIS) is also a key parameter to determine the performance of all-solid-state supercapacitors. Figure 4f show the Nyquist plots in the frequency range from 100 KHz to 0.1 Hz. Typically, the Nyquist plot can be divided into a high frequency semicircle and a low frequency vertical line, the semicircle intersection with the abscissa depends on the internal resistance, and the vertical line implies good capacitive behaviors of supercapacitors.<sup>34,37</sup> As can be seen from Figure 4f, the approximate nonexistence of the semicircle in the high-frequency region illustrates good charge transfer conductivity of the device at the electrolyte-electrode interface.<sup>1</sup>

For the practical applications, self-discharge and leakage current are important references of the flexible device. As shown in Figure 5a, the leakage current dropped quickly in the beginning and then tended to become stable finally (4.66 μA). Such small value of leakage current, which is ascribed to the self-discharge course in the device, means less shuttle reactions caused by the impurities in the electrode materials.<sup>3,7,8</sup> Figure 5b shows the time courses of the open-circuit voltage. It undergoes rapid self-discharge course in several minutes. However the discharge process is limited after several hours. The flexible device shows a stable output voltage of about 0.288 V after 4 h and almost 40 % of the initial charged potential is retained even after 10 h.<sup>3</sup>

The symmetrical flexible all-solid-state SC was fabricated by sandwiching poly KOH/PVA gel between two NiO@C cloth electrodes, and the model of the device has been given in the left bottom of Figure 6a. To demonstrate the potential uses of the flexible device, two of the same units with activated area 3.5 cm<sup>2</sup> were connected in series. After charging for the tandem devices at 1mA/cm<sup>2</sup>, it can power a red LED for several seconds.

Long-term cycling stability of the flexible device at a current density of  $1 \text{ mA/cm}^2$  for up to 10000 cycles was also tested. The specific capacitance as function of the cycle number is depicted in Figure 6b. From the image, we can clearly know that the charge/discharge process mainly includes two stages: the activation period and the stable stage. As the electrolyte gradually penetrates into the whole surface of the electrodes, the sufficiently activated materials cause the capacitance increasing from  $11.36 \text{ mF/cm}^2$  to  $20 \text{ mF/cm}^2$ , and then maintain at  $20 \text{ mF/cm}^2$  without obvious capacitance fading in the following cycles.<sup>38</sup>

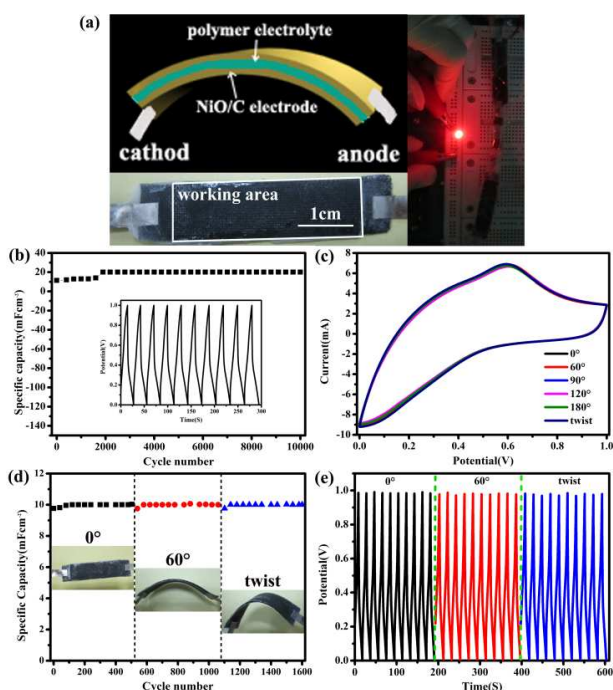


**Figure 6.** (a) Optical photographs of the fabricated flexible all-solid-state supercapacitor device. The left bottom image shows the model of the device. The square of the left down picture indicates the capacitance region. The right image shows a light-emitting diode (LED) turned on by the NiO/C cloth based flexible supercapacitors. (b) Capacitance retention over 10000 cycles of charge-discharge at a current density of  $1 \text{ mA/cm}^2$ . The insert picture shows the first 10 cycles. (c) Cyclic voltammetry curves for the flexible supercapacitors at different curvature of  $0^\circ$ ,  $60^\circ$ ,  $90^\circ$ ,  $120^\circ$ ,  $180^\circ$  and twist with a scan rate of  $100 \text{ mV/s}$ . (d) Specific capacitance over 500 cycles under the curvature of  $0^\circ$ ,  $60^\circ$ , and twist at current density of  $1 \text{ mA/cm}^2$ . (e) The first 10 cycles of the curvature of  $0^\circ$ ,  $60^\circ$ , and twist.

To evaluate the feasibility of the flexible all-solid-state NiO/C cloth SCs for flexible energy storage device, we also test the CV property under different curvature conditions. Figure 6c depicted that the different bending angles ( $60^\circ$ ,  $90^\circ$ ,  $120^\circ$ ,  $180^\circ$  and twist) lead little change to the CV curves, conforming that the device has outstanding mechanical flexibility. The electrochemical stability of the flexible all-solid state of NiO/C cloth SCs was examined at a scan rate of  $100 \text{ mV/s}$ .<sup>39</sup> The cycle stability under severe condition is also an important parameter to study the flexible device. Under the curvature of  $0^\circ$ ,  $60^\circ$  and twisted condition, over 500 cycles at the current density of  $1 \text{ mA/cm}^2$  were test respectively, and the results is shown in Figure 6d. By comparing the specific capacitance at  $60^\circ$  bend and twist condition with normal state,

we can draw a conclusion that the curvature of  $60^\circ$  and twist condition do little harmful to the flexible SC device, which further demonstrate the device with excellent mechanical stability.<sup>36,40</sup> What's more, the first 10 cycles of the charge/discharge voltage curve under the curvatures of  $0^\circ$ ,  $60^\circ$  and twist condition are given in Figure 6e. Remarkably, the specific capacitance of device at normal state matches well with that under  $60^\circ$  and twist conditions.

## Conclusions

In summary, we have created a simple method to grow NiO on carbon cloth by utilizing pre-grown ZnO nanoparticles as the buffer layer. The as-synthesized NiO/C cloth electrode shows a high specific capacitance and excellent cycling stability when applied in the three-electrode system. In view of practical application, we fabricated flexible all-solid-state supercapacitors with two strips of symmetric NiO/C cloth electrodes, and KOH/PVA gel was brought in as electrolyte and separator. The entire device exhibits remarkable electrochemical performances, such as high capacitance, high flexibility, long lifetime and good stability. Furthermore, it can power a red commercial light-emitting-diode (LED). Working at awful conditions, the flexible device still presents good capacitance stability. Our work not only opens up a possibility to engineer NiO into a promising pseudocapacitive material but also highlights the path for next generation flexible energy storage devices.

## Acknowledgements

This work was supported by the National Natural Science Foundation (61377033, 91123008), the Program for National Basic Research Program of China (grant no. 2011CB933300), the Program for New Century Excellent Talents of the University in China (grant no. NCET-11-0179), the Fundamental Research Funds for the Central Universities (HUST: 2013NY013) and Wuhan Science and Technology Bureau (20122497).

## Notes and references

- <sup>a</sup> Wuhan National Laboratory for Optoelectronics (WNLO), Huazhong University of Science and Technology (HUST), Wuhan 430074, China. E-mail: dichen@mail.hust.edu.cn
- <sup>b</sup> State Key Laboratory for Superlattices and Microstructures, Institute of Semiconductors, Chinese Academy of Sciences, Beijing 100083, China. E-mail: gzshen@semi.ac.cn

† Electronic Supplementary Information (ESI) available: [SEM image and XRD pattern of the products without ZnO buffer layer, Electrochemical properties of the NiO/ZnO on carbon cloth, SEM image and XRD pattern of the sample after cycled for 1000 times]. See DOI: 10.1039/b000000x/

‡ Y. Qian and R. Liu contributed equally to this work.

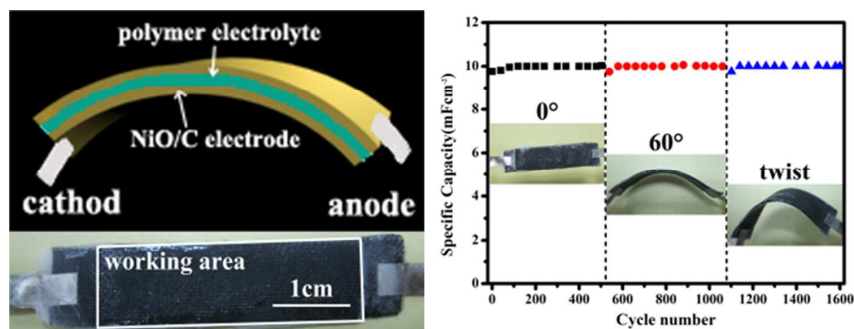
- J. Xu, Q. F. Wang, X. W. Wang, Q. Y. Xiang, B. Liang, D. Chen and G. Z. Shen, *ACS Nano*, 2013, **7**, 5453–5462.
- W. Chen, R. B. Rakhi, L. B. Hu, X. Xie, Y. Cui and H. N. Alshareef, *Nano Lett.* 2011, **11**, 5165–5172.

- 3 L. Yang, S. Cheng, Y. Ding, X. B. Zhu, Z. L. Wang and M. L. Liu, *Nano Lett.*, 2012, **12**, 321–325.
- 4 L. L. Zhang, X. Zhao, M. D. Stoller, Y. W. Zhu, H. X. Ji, S. Murali, Y. P. Wu, S. Perales, B. Clevenger and R. S. Ruoff, *Nano Lett.*, 2012, **12**, 1806–1812.
- 5 H. L. Wang, C. M. B. Holt, Z. Li, X. H. Tan, B. S. Amirkhiz, Z. W. Xu, B. C. Olsen, T. Stephenson and D. Mitlin, *Nano Res.*, 2012, **5(9)**: 605–617.
- 6 X. H. Lu, G. M. Wang, T. Zhai, M. H. Yu, S. L. Xie, Y. C. Ling, C. L. Liang, Y. X. Tong and Y. Li, *Nano Lett.*, 2012, **12**, 5376–5381.
- 7 Q. F. Wang, X. F. Wang, B. Liu, G. Yu, X. J. Hou, D. Chen and G. Z. Shen, *J. Mater. Chem. A*, 2013, **1**, 2468–2473.
- 8 X. F. Wang, B. Liu, Q. F. Wang, W. F. Song, X. J. Hou, D. Chen, Y. B. Cheng and G. Z. Shen, *Adv. Mater.*, 2013, **25**, 1479–1486.
- 15 H. M. Zheng, T. Zhai, M. H. Yu, S. L. Xie, C. L. Liang, W. X. Zhao, S. C. I. Wang, Z. S. Zhang and X. H. Lu, *J. Mater. Chem. C*, 2013, **1**, 225–229.
- 10 C. Z. Meng, C. H. Liu, L. Z. Chen, C. H. Hu and S. S. Fan, *Nano Lett.*, 2010, **10**, 4025–4031.
- 11 H. C. Gao, F. Xiao, C. B. Ching and H. W. Duan, *ACS Appl. Mater. Interfaces*, 2012, **4**, 7020–7026.
- 12 Z. S. Wu, Y. Sun, Y. Z. Tan, S. B. Yang, X. L. Feng and K. Müllen, *J. Am. Chem. Soc.*, 2012, **134**, 19532–19535.
- 25 13 Y. H. Xiao, A. Q. Zhang, S. J. Liu, J. H. Zhao, S. M. Fang, D. Z. Jia and F. Li, *Journal of Power Sources*, 2012, **219**, 140–146.
- 14 M. Yang, J. X. Li, H. H. Li, L. W. Su, J. P. Wei and Z. Zhou, *Phys. Chem. Chem. Phys.*, 2012, **14**, 11048–11052.
- 15 C. Z. Yuan, X. G. Zhang, L. H. Su, B. Gao and L. F. Shen, *J. Mater. Chem.*, 2009, **19**, 5772–5777.
- 30 16 B. Wang, J. S. Chen, Z. Y. Wang, S. Madhavi and X. W. (David) Lou, *Adv. Energy Mater.*, 2012, **2**, 1188–1192.
- 17 B. Liu, J. Xu, S. H. Ran, Z. R. Wang, D. Chen and G. Z. Shen, *CrystEngComm*, 2012, **14**, 4582–4588.
- 35 18 W. J. Zhou, X. H. Cao, Z. Y. Zeng, W. H. Shi, Y. Y. Zhu, Q. Y. Yan, H. Liu, J. Y. Wang and H. Zhang, *Energy & Environmental Science*, DOI: 10.1039/C3EE40155C.
- 19 R. Kozhummal, Y. Yang, F. Guder, A. Hartel, X. L. Lu, U. M. Ku'c-u'kbayrak, A. Mateo-Alonso, M. Elwenspoek and M. Zacharias, *ACS Nano*, 2012, **6**, 7133–7141.
- 40 20 J. Xu, H. Wu, C. Xu, H. T. Huang, L. F. Lu, G. Q. Ding, H. L. Wang, D. F. Liu, G. Z. Shen, D. D. Li and X. Y. Chen, *Chem. Eur. J.*, 2013, **19**, 6451–6458.
- 21 Q. F. Wang, J. Xu, X. F. Wang, B. Liu, X. J. Hou, G. Yu, P. Wang, D. Chen and G. Z. Shen, *ChemElectroChem*, 2014, **1**, 559–564.
- 45 22 J. Feng, X. Sun, C. Z. Wu, L. L. Peng, C. W. Lin, S. L. Hu, J. L. Yang and Y. Xie, *J. Am. Chem. Soc.*, 2011, **133**, 17832–17838.
- 23 X. H. Lu, G. M. Wang, T. Zhai, M. H. Yu, S. L. Xie, Y. C. Ling, C. L. Liang, Y. X. Tong and Y. Li, *Nano Lett.*, 2012, **12**, 1690–1696.
- 50 24 J. P. Liu, J. Jiang, M. Bosman and H. J. Fan, *J. Mater. Chem.*, 2012, **22**, 2419–2426.
- 25 X. C. Dong, X. W. Wang, J. Wang, H. Song, X. G. Li, L. H. Wang, M. B. C.-Park, C. M. Li and P. Chen, *Carbon*, 2012, **50**, 4865–4870.
- 55 26 J. W. Leea, T. Ahna, J. H. Kima, J. M. Kob and J. D. Kim, *Electrochimica Acta*, 2011, **56**, 4849–4857.
- 27 P. Lv, Y. Y. Feng, Y. Li and W. Feng, *Journal of Power Sources*, 2012, **220**, 160–168.
- 60 28 M. Qaid, I. P. Radu, D. J. Cott, M. AlSalhi and P. M. Vereecken, *IMEC*, 2012.
- 29 C. S. Du and N. Pan, *Nanotechnology*, 2006, **17**, 5314–5318.
- 30 K. Z. Gao, Z. Q. Shao, J. Li, X. Wang, X. Q. Peng, W. J. Wang and F. J. Wang, *J. Mater. Chem. A*, 2013, **1**, 63–67.
- 65 31 Y. W. Cheng, S. T. Lu, H. B. Zhang, C. V. Varanasi and J. Liu, *Nano Lett.*, 2012, **12**, 4206–4211.
- 32 C. Zhou, Y. W. Zhang, Y. Y. Li and J. P. Liu, *Nano Lett.*, 2013, **13**, 2078–2085.
- 70 33 X. F. Wang, B. Liu, R. Liu, Q. F. Wang, X. J. Hou, D. Chen, R. M. Wang and G. Z. Shen, *Angew. Chem. Int. Ed.*, 2014, **53**, 1849–1853.
- 34 D. W. Wang, Q. H. Wang and T. M. Wang, *Ionics*, 2013, **19**, 559–570, DOI 10.1007/s11581-012-0781-1.
- 75 35 J. L. Xue, Y. Zhao, H. H. Cheng, C. G. Hu, Y. Hu, Y. N. Meng, H. B. Shao, Z. P. Zhang and L. T. Qu, *Phys. Chem. Chem. Phys.*, 2013, **15**, 8042–8045.
- 36 L. N. Gao, X. F. Wang, Z. Xie, W. F. Song, L. J. Wang, X. Wu, F. Y. Qu, D. Chen and G. Z. Shen, *J. Mater. Chem. A*, 2013, **1**, 7168–7173.
- 80 37 D. P. Dubal and R. Holze, *Energy*, 2013, **51**, 407–412.
- 38 Z. S. Wu, A. Winter, L. Chen, Y. Sun, A. Turchanin, X. L. Feng and K. Müllen, *Adv. Mater.*, 2012, **24**, 5130–5135.
- 39 B. G. Choi, J. Hong, W. H. Hong, P. T. Hammond, and H. Park, *ACS Nano*, 2011, **5**, 7205–7213.
- 85 40 Y. J. Kang, H. Chung, C. H. Han and W. Kim, *Nanotechnology*, 2012, **23**, 289501 (1pp).

# Efficient synthesis of hierarchical NiO nanosheets for high-performance flexible all-solid-state supercapacitor

Yue Qian,<sup>a</sup> Rong Liu,<sup>a</sup> Qiufan Wang,<sup>a</sup> Jing Xu,<sup>a</sup> Di Chen<sup>\*,a</sup> and Guozhen Shen<sup>\*,b</sup>

## Table of Content image and text



A simple strategy was developed to grow NiO nanosheets on carbon cloth as a binder-free electrode for high-performance flexible all-solid-state supercapacitor device.